remote sensing

MDPI

Article

A Novel Mine-Specific Eco-Environment Index (MSEEI) for Mine Ecological Environment Monitoring Using Landsat Imagery

Peipei Zhang [1,2], Xidong Chen [2,*], Yu Ren [3], Siqi Lu [4], Dongwei Song [5] and Yingle Wang [6]

[1] Henan Institute of Surveying and Mapping, Zhengzhou 450003, China
[2] College of Surveying and Mapping and Geographic Information, North China University of Water Resources and Electric, Zhengzhou 450045, China
[3] College of Geography and Environmental Science, Northwest Normal University, Lanzhou 730070, China
[4] Department of Geography, University of Connecticut, Storrs, CT 06269-4148, USA
[5] No.7 Geological Party, Henan Nonferrous Metals Geological and Mineral Bureau, Zhengzhou 450016, China
[6] Henan Institue of Remote Sensing and Geomatics, Zhengzhou 450003, China
* Correspondence: chenxd@radi.ac.cn; Tel.: +86-158-2755-9609

Abstract: The excessive exploitation of mineral resources will lead to environmental pollution, resource depletion, environmental disaster, and other problems. The contradiction between the environment and development, and the management of the ecological environment in mining areas are urgent *p*-problems to be solved. An ecological environment assessment is an important part of the ecological environment in a mining area. The accurate evaluation of the ecological environment is the premise behind environmental governance in a mining area. However, current ecological assessment indicators were not developed specifically for mine environment monitoring and, thus, cannot provide an effective and comprehensive assessment of the mineral environment. To this end, in order to improve the environmental monitoring performance in mining areas, a novel Mine-Specific Eco-Environment Index (MSEEI) was proposed, integrating factors from five main aspects associated with minerals, including temperature, vegetation, soil moisture, atmospheric environment, and mining scale. Meanwhile, a widely concerned mine—Luanchuan mine—was used as the case area to test the performance of our MSEEI. The results showed a significant correlation between RSEI and MSEEI ($p < 0.01$). The mean correlation achieved between RSEI and MSEEI was 0.91, which was much higher than the correlations between RSEI and enhanced vegetation index (EVI), soil moisture monitoring index (SMMI), normalized difference built-up and soil index (NDBSI), PM2.5 concentration (DI), and heat (LST). In addition, based on our long-term MSEEI results of Luanchuan mine from 1997 to 2021, the ecological status of Luanchuan mine showed a trend of first declining and then rising. Specifically, the MSEEI first declined from 0.85 to 0.77 between 1997 and 2012, and then rebounded to about 0.8 in recent years. The MSEEI exhibited a good applicability in the ecological assessment of mining areas. Our MSEEI can provide useful guidance for mine environment monitoring. MSEEI can directly reflect the ecological damage after mining, provide scientific guidance for the exploitation and utilization of mineral resources, and promote the protection and sustainable development of Earth's resources and mine ecological environments.

Keywords: Mine-Specific Eco-Environment Index (MSEEI); mining area; ecological assessment; remote sensing

check for updates

Citation: Zhang, P.; Chen, X.; Ren, Y.; Lu, S.; Song, D.; Wang, Y. A Novel Mine-Specific Eco-Environment Index (MSEEI) for Mine Ecological Environment Monitoring Using Landsat Imagery. *Remote Sens.* **2023**, *15*, 933. https://doi.org/10.3390/rs15040933

Academic Editor: Alfredo Huete

Received: 15 November 2022
Revised: 27 January 2023
Accepted: 1 February 2023
Published: 8 February 2023

Copyright: © 2023 by the authors. Licensee MDPI, Basel, Switzerland. This article is an open access article distributed under the terms and conditions of the Creative Commons Attribution (CC BY) license (https://creativecommons.org/licenses/by/4.0/).

1. Introduction

According to the 2021 China Mineral Resources Report, by the end of 2020, China had discovered 173 minerals, including 13 energy minerals, 59 metal minerals, 95 non-metallic minerals, and 6 water and gas minerals (2011–2020). The proven geological reserves of oil and natural gas newly added within ten years total 10.1 billion tons and 6.85 trillion cubic meters, respectively, accounting for about 25% and 45%, respectively, of the cumulative proven total since the founding of New China.

Ecological protection is inseparable from the development of mineral resources. The excessive exploitation of mineral resources aggravates the destruction of the ecological environment and produces a series of ecological and environmental problems, such as frequent geological disasters, a fragile ecological carrying capacity, surface subsidence, vegetation destruction, groundwater resource and environmental damage, dust pollution, and land degradation [1–6]. Since 2020, the central government has allocated CNY 2 billion in two batches to support 12 provinces (autonomous regions) in carrying out the ecological restoration and treatment of historical mines in the Yellow River Basin and the Qinghai Tibet Plateau, and to solve the problems of historical mines, which play important roles in ensuring national ecological security, providing a wide range of ecological benefits, and maintaining production and quality of life. According to remote sensing monitoring data, about 41,600 hectares of new mines will be restored and managed in 2020. The area under construction and restoration is about 117,000 hectares, accounting for about 11,000 hectares, and the newly restored area of abandoned mines is about 30,500 hectares, accounting for 73.3%.

The evaluation and prediction of the ecological environment of a mining area are important parts of research on the ecological environment of the mining area, and it is also the premise behind the environmental protection and management of the mining area. Remote sensing technology has become an important means of monitoring the ecological environment of the mining area [7–12] and the progress in quantitative remote sensing monitoring research on the ecological environment of mining areas at home and abroad [13]. The quantitative monitoring of surface elements of the ecological environment in mining areas mainly includes quantitative remote sensing monitoring of vegetation, soil, water, atmospheric environment, and ecosystem parameters. The current research on remote sensing monitoring of ecosystem parameters in mining areas mainly focuses on ecosystem carbon sequestration, ecosystem service value, the Remote Sensing Ecology Index (RSEI) [14–23], the landscape index, etc. The remote sensing monitoring of the carbon sequestration capacity of a mining area ecosystem focuses on calculating the vegetation carbon sink and soil carbon sequestration in the mining area, and monitoring the carbon sequestration capacity of the mining area ecosystem. Ecosystem Product (GEP) accounting reveals the temporal and spatial variation in the value of ecosystem services in mining areas. Since the Remote Sensing Ecological Index (RSEI) [24] was proposed by Xu Hanqiu of Fujian University, the index has been widely used in the monitoring of the ecological environment quality of mining areas. Some researchers directly calculate the RSEI in a mining area and determine the RSEI value of the mining area. The spatial and temporal changes of a mining area can be analyzed, in order to monitor changes in the quality of the ecological environment in the mining area. The remote sensing monitoring of the mining area landscape index mainly uses remote sensing data to calculate the mining area landscape index, and then analyzes the temporal and spatial changes in the mining area landscape pattern.

This study aims to use long time series remote sensing images to retrieve multiple parameters related to mine ecological environments, and to couple multiple parameters into a parameter suitable for mine ecological evaluation to evaluate the long time series ecological environment of a mining area, to provide scientific guidance for the development and utilization of mineral resources, and to promote the protection and sustainable development of Earth's resources and mine ecological environments.

In this study, we considered the effects of vegetation degradation, topographical changes, soil moisture content reduction, and the fugitive dust generated during open-pit mining perforation construction and transportation on the ecological environment that may be caused by mining activities based on the remote sensing data inversion of the enhanced vegetation index (EVI), the soil moisture monitoring index (SMMI), the normalized difference built-up and soil index (NDBSI), the PM2.5 concentration (DI), and heat (LST) in the mining area. EVI, SMMI, NDBSI, DI, and LST were coupled together to establish the Mine-Specific Eco-Environment Index (MSEEI). The MSEEI in the Luanchuan

mining area from 1997 to 2021 was compared and analyzed from the two dimensions of time and space; the spatial coupling relationship between the ecological changes in the mining area, the type of mine occupation, and the distribution of mining sites was further analyzed, and the impact of ecological changes in the MSEEI mining area was discussed. The MSEEI was constructed according to the construction method of the RSEI model, which is suitable for the ecological environment evaluation of a mining area. The research results reflect the ecological status of the Luanchuan mining area in a long time series and provide accurate data supporting the formulation of ecological plans in subsequent mining areas.

2. Materials and Methods

2.1. Study Area

Luanchuan mine concentration area is located in the East Qinling Mountains. It covers an area of 247.82 square kilometers and is made up of 46 mines (including gold, pyrite, molybdenum, iron, lead, zinc mines) and 4 major sub-mining areas built in 1997 and before (Figure 1). The Luanchuan mining area has the title of "Molybdenum Capital of the World" and produces Nannihu-Sandaozhuang-Shangfang Large-Super Large Porphyry-Xika Rock Molybdenum (Tungsten) Deposits, as well as Large Lead-Zinc-Silver Polymetallic Deposits of Camel Mountain, Cold Water, and Laterite Shop. Since the Neoproterozoic, Luanchuan mine concentration area has undergone many complex structural and property changes. As a result, the tectonic traces of the Luanchuan mine concentration area are widely developed in different directions. In the development of mineral resources, Luanchuan mine concentration area is in the extensive mining mode of high pollution and high consumption. Due to the lack of relevant laws and regulations on mine environmental protection and governance, the overall mine ecological environment was reported in a deteriorating state. Therefore, choosing Luanchuan mine concentration area as the study area is of great significance for the environmental monitoring and protection of Luanchuan mine.

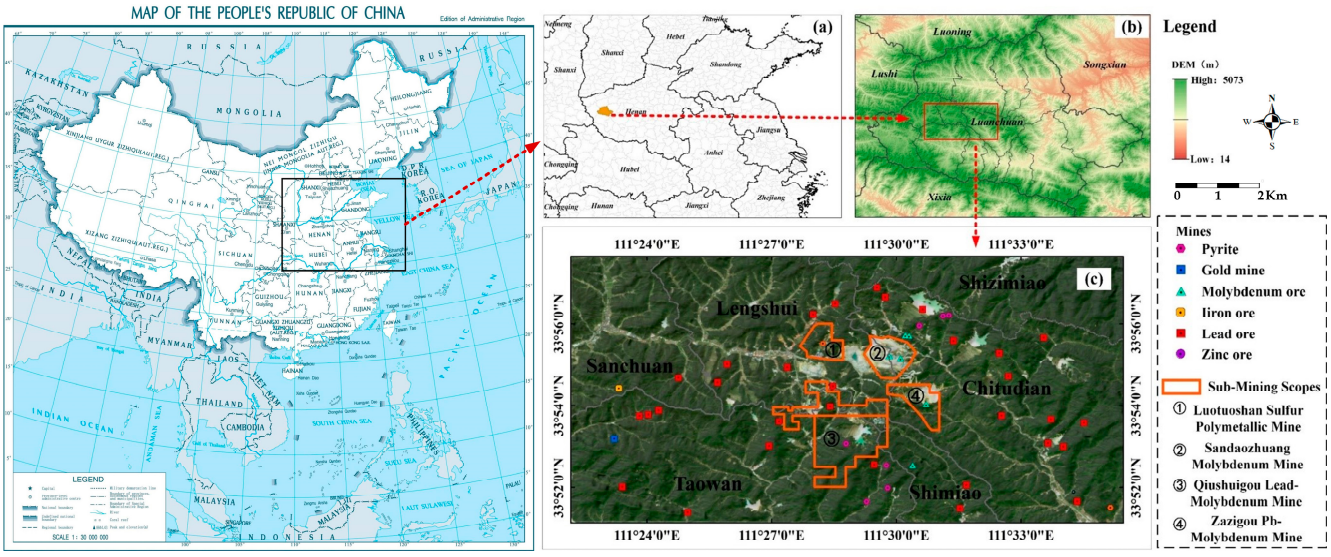


Figure 1. Location of Luanchuan County, Luoyang City, Henan Province (**a**); location of the Luanchuan mining concentration area (**b**); mine distribution location of Luanchuan mining concentration area (**c**).

2.2. Materials

In order to assess the long-term variation in the ecological environment of Luanchuan mine, all Landsat series Level-1 precision terrain (L1TP) surface reflectance imagery of the Luanchuan mine, including Landsat 5, Landsat 7, and Landsat 8 imagery, from 1997 to 2021, were collected via the United States Geological Survey (https://www.usgs.gov/, accessed on 17 September 2022). Furthermore, taking into account the interference of clouds

and cloud shadows, Landsat images from every three years were used to composite the corresponding cloud-free images for analysis. The median composition method was used to generate cloud-free images [25]. As a result, a total of 9 cloud-free images (for the year of 1997, 2000, 2003, 2006, 2009, 2012, 2015, 2018, and 2021) were generated in our study. The spatial analysis and mapping tools of arcgis10.6 were used for mapping expression and statistical analysis of the MSEEI.

2.3. Mine-Specific Eco-Environment Index (MSEEI)

Although several ecology assessment indicators were proposed over the past years, they were not developed specifically for mine environment monitoring, and thus do not include sufficient factors associated with the environment of mining areas. Taking into account that mining activities can cause vegetation destruction, soil drying, air pollution, and abnormal surface temperatures [26,27], the enhanced vegetation index (EVI) [28], soil moisture monitoring index (SMMI) [29], difference index (DI) [30], and Land Surface Temperature (LST) [31] can reflect the above issues, respectively. Therefore, the EVI, SMMI, DI, and LST were selected to monitor the greenness, soil moisture, air pollution, and the surface temperature of the mine, respectively. Additionally, since expansion of a mining area also exacerbates the aforementioned environmental issues, the normalized difference built-up and soil index (NDBSI) [32], which can monitor the scale of a mining area, was also used to develop our MSEEI. In the end, a total of 5 indicators (EVI, SMMI, DI, LST, and NDBSI) were selected to make up our MSEEI (Figure 2).

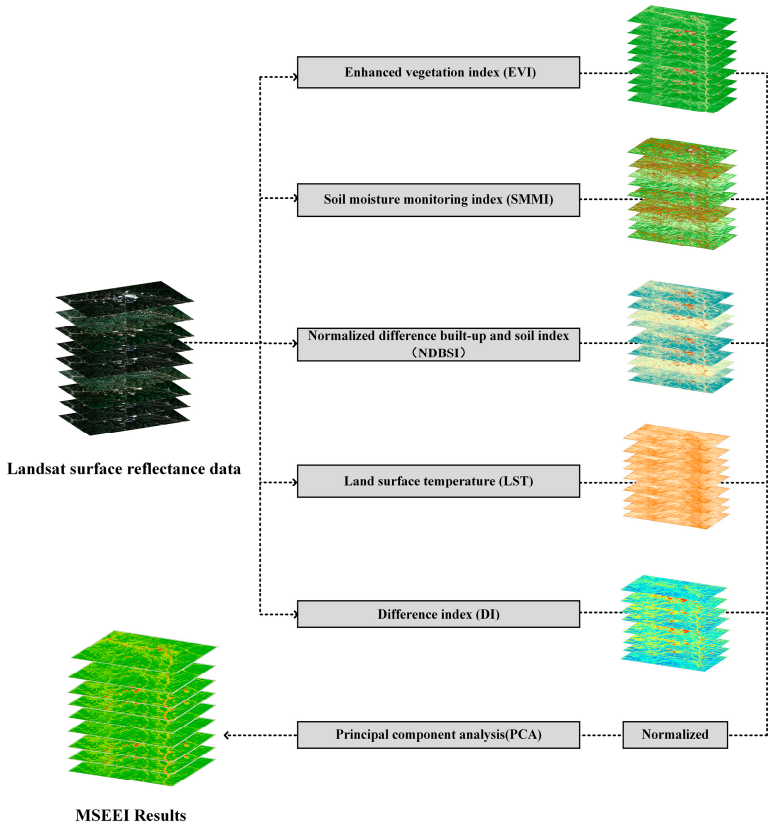


Figure 2. Flowchart of our MSEEI method.

Referring to the method of the RSEI [33], principal component analysis (PCA) [34] was used to couple the five indicators (EVI, SMMI, NDBSI, DI, and LST). Their weights were determined based on the original data characteristics of the indicators, which helps avoid uncertainty in the determination of their weights due to human influence, and is easy to operate. Since the unit and data ranges between the five indicators were not uniform, it

was necessary to normalize these indicators between 0 and 1 before performing principal component analysis.

Principal component transformation was used to integrate the above five indicators, and the weights were automatically and objectively determined according to the contribution of each indicator to the principal component, in order to realize the purpose of coupling multiple indicators with a single variable. PC1 is the first principal component of the principal component analysis results. It represents the indicator with the greatest variance that can best explain the state of the environment among the environmental indicators (EVI, SMMI, NDBSI, DI, and LST). When PC1 has a low value in areas with good ecological quality and a high value in areas with poor environmental quality, PC1 needs to be subtracted from one so that the high value represents good ecological condition:

$$\mathrm{MSEEI_l} = 1 - \mathrm{PC1}[\mathrm{f}(\mathrm{EVI}, \mathrm{SMMI}, \mathrm{NDBSI}, \mathrm{DI}, \mathrm{LST})] \quad (1)$$

$$\mathrm{MSEEI} = (\mathrm{MSEEI_l} - \mathrm{MSEEI_{min}})/(\mathrm{MSEEI_{max}} - \mathrm{MSEEI_{min}}) \quad (2)$$

where $\mathrm{MSEEI_{min}}$ and $\mathrm{MSEEI_{max}}$ are the minimum and maximum values of the index, respectively.

During mining, a large number of forests are cut down, and grasslands are damaged. Vegetation coverage is a key indicator of ecological environment monitoring in mining areas; the size of the enhanced vegetation index value directly reflects the vegetation area in the target area [35]:

$$\mathrm{EVI} = 2.5 \times \frac{\mathrm{N} - \mathrm{R}}{\mathrm{N} + 6 \times \mathrm{R} - 7.5 \times \mathrm{B} + 1} \quad (3)$$

where N and R represent the near-infrared and red bands of Landsat 5 TM, Landsat 7 ETM, and Landsat 8 OLI/TIRS, respectively.

The continuous drainage and drainage of groundwater in the underground mining mode adopted by some mining areas causes the groundwater level in the area to drop, disrupting the balance of water resources in the mining area; this leads to a shortage of common water resources. In order to reflect the water-holding capacity of the soil in the mining area, the SMMI (Soil Moisture Monitoring Index) was constructed to reflect the water content of the soil in the Luanchuan mining area [36]:

$$\mathrm{SMMI} = \sqrt{\mathrm{R}^2 + \mathrm{N}^2}/\sqrt{2} \quad (4)$$

where N and R represent the near-infrared and red bands of Landsat 5 TM, Landsat 7 ETM, and Landsat 8 OLI/TIRS, respectively.

Land resources are directly occupied or indirectly damaged due to mining, due to tailings and waste rock accumulation and other factors, and land cover is replaced by open pits, concentrators, waste dumps, and waste rock heaps. We chose the average value of the NDBSI to express this ecological situation. The NDBSI is the average of bare soil index SI and building index IBI [32]:

$$\mathrm{NDBSI} = (\mathrm{SI} + \mathrm{IBI})/2 \quad (5)$$

$$\mathrm{SI} = \frac{(\mathrm{S_1} + \mathrm{R}) - (\mathrm{B} + \mathrm{N})}{(\mathrm{S_1} + \mathrm{R}) + (\mathrm{B} + \mathrm{N})} \quad (6)$$

$$\mathrm{IBI} = \frac{2\mathrm{S_1}/(\mathrm{S_1} + \mathrm{N}) - (\mathrm{N}/(\mathrm{N} + \mathrm{R}) + \mathrm{G}/(\mathrm{G} + \mathrm{S_1}))}{2\mathrm{S_1}/(\mathrm{S_1} + \mathrm{N}) + (\mathrm{N}/(\mathrm{N} + \mathrm{R}) + \mathrm{G}/(\mathrm{G} + \mathrm{S_1}))} \quad (7)$$

where R, G, B, N, and $\mathrm{S_1}$ represent the red, green, blue, near-infrared, shortwave infrared, and red bands of Landsat 5 TM, Landsat 7 ETM, and Landsat 8 OLI/TIRS, respectively.

Due to the damage and destruction of landform and land resources, a large amount of dust has been dispersed. According to the PM2.5 of particles, the reflectivity of the red band increases, and the reflectivity of near-infrared band decreases. The difference index (DI) is used to characterize the change in particle concentration [30]:

$$\mathrm{DI} = \mathrm{R} - \mathrm{N} \quad (8)$$

where N and R represent the near-infrared and red bands of Landsat 5 TM, Landsat 7 ETM, and Landsat 8 OLI/TIRS, respectively.

Mining activities will cause the surface temperature in the mining area to be higher than that in non-mining areas. We chose the surface temperature LST to reflect this surface temperature anomaly [37]:

$$L = \text{gain} \times DN + \text{bias} \tag{9}$$

$$T = K_2 / \ln(K_1 / L + 1) \tag{10}$$

$$LST = T / [1 + (\lambda T / \rho) \ln \varepsilon] \tag{11}$$

where L is the temperature value of the thermal infrared band at the sensor; gain is the gain value; DN is the gray value of the pixel; bias is the bias value; T is the temperature value at the sensor; K = 774.89 W/(m^2·sr·μm); K_2 = 1321.08 K; λ is the central wavelength of the thermal infrared band; ρ is 1.438 × 10^{-2} m·K; ε is the specific emissivity of ground objects estimated by the NDVI according to Sobrino's model.

2.4. Validating the MSEEI

In this study, we evaluated the performance of the MSEEI by comparing its results with those of the RSEI, another environmental degradation index. The RSEI couples the greenness, humidity, dryness, and heat indicators that reflect the ecological environment, which can monitor and evaluate the quality of the regional ecological environment. In the present study, the average degree of correlation was used, which indicates the overall representativeness of the MSEEI and the correlation among the various indicators. It can be expressed as follows:

$$\overline{R} = \sum_{i=1}^{n} |R_i| / n \tag{12}$$

where n is the number of indicators, and R_i is the correlation coefficient between each indicator and the MSEEI.

2.5. Kernel Density Analysis and Fractal Dimension Statistics

Using the method of combining kernel density analysis and data grids, the RSEI and the mining points are gridded to analyze the relationship between the mining points and ecological changes. Kernel density analysis technology can achieve accurate and high-quality probability density estimation for point data, and it is an effective method for probability density estimation for mine point data:

$$f(s) = \frac{1}{h} \sum_{i=0}^{n} K\left[\frac{D(S, S_i)}{h}\right] \tag{13}$$

where n can represent the number of vector spaces and entities that need to be included in the value range of the average distance between two points. K() can be used to directly represent a kernel computing function, and it generally can be used to represent a kernel computing function using a quartic polynomial. h is the distance threshold (bandwidth), which represents the Euclidean average distance between two points. Fractal dimension statistics of the change values of the mine site and the MSEEI further explore changes in the mine site and MSEEI.

3. Results

3.1. MSEEI Performance Validation

We conducted statistics on the occurrence frequency of ecological state values of the RSEI and MSEEI (Figure 3). Trends in ecological value distribution curves of the RSEI and MSEEI are consistent, indicating that the MSEEI can well reflect the overall ecological status of mining areas.

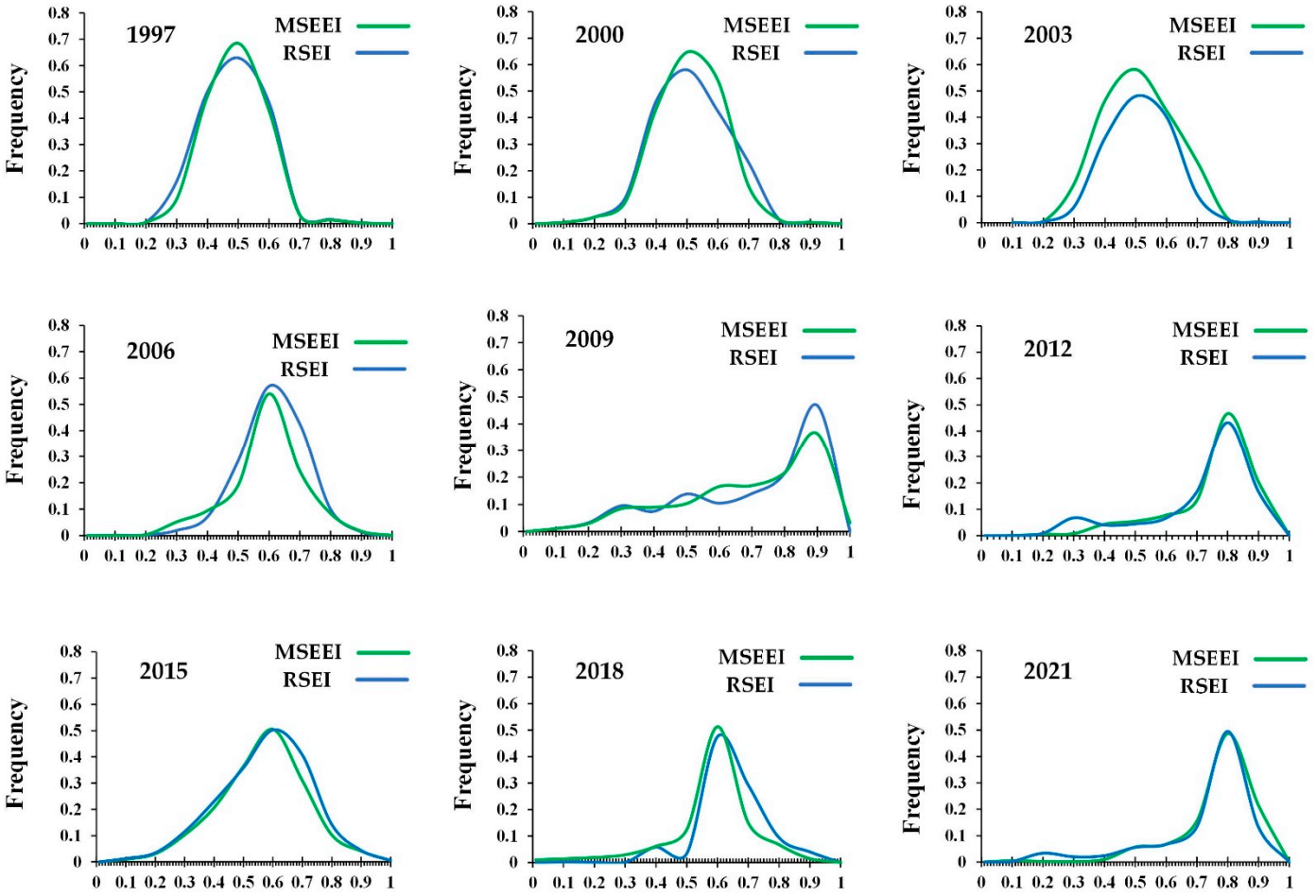


Figure 3. RSEI and MSEEI index frequencies in 1997, 2000, 2003, 2006, 2009, 2012, 2015, 2018, and 2021.

We calculated RSEI and MSEEI correlations for nine years; the correlation values are 0.867 ($p < 0.01$), 0.875 ($p < 0.01$), 0.879 ($p < 0.01$), 0.861 ($p < 0.01$), 0.871 ($p < 0.01$), 0.867 ($p < 0.01$), 0.859 ($p < 0.01$), 0.864 ($p < 0.01$), and 0.901 ($p < 0.01$) (Figure 4).

The average correlations (Table 1) between the MSEEI and EVI, SMMI, NDBSI, DI, and LST in 1997, 2000, 2003, 2006, 2009, 2012, 2015, 2018, and 2021 were compared. The average correlation of the MSEEI with the EVI, SMMI, NDBSI, DI, and LST range from 0.773 to 0.968. The EVI had the highest average correlation among indicators, the average of the nine years was 0.863, and the average correlation of the MSEEI was 0.910, which was 5.4% higher than the EVI, indicating that the MSEEI was more suitable than any single indicator to characterize the ecological environment.

The average MSEEI values (Table 2) shown above in the nine years were 0.85 (1997), 0.82 (2000), 0.83 (2003), 0.81 (2006), 0.79 (2009), 0.77 (2012), 0.80 (2015), 0.84 (2018), and 0.80 (2021). The average MSEEI in nine years was between 0.77 and 0.85, indicating that the quality of the ecological environment in the Luanchuan mining concentration area remained unchanged from 1997 to 2021. At the "better" level, the MSEEI value increased with an increase in EVI indicators that had a positive impact on the ecological status, and decreased with an increase in the NDBSI, DI, and LST indicators that had a negative impact on the ecological status. EVI had the most direct impact on the MSEEI among the five single indicators. The average values of EVI indicators that had a positive impact on the ecological status of the study area show a trend of "decline-up-decline-up"; specifically, the EVI first declined from 0.916 to 0.831 between 1997 and 2003, and then rebounded to about 0.887 in 2009; the EVI next declined from 0.887 to 0.815 between 2009 and 2015, and then rebounded to about 0.871 in 2021.

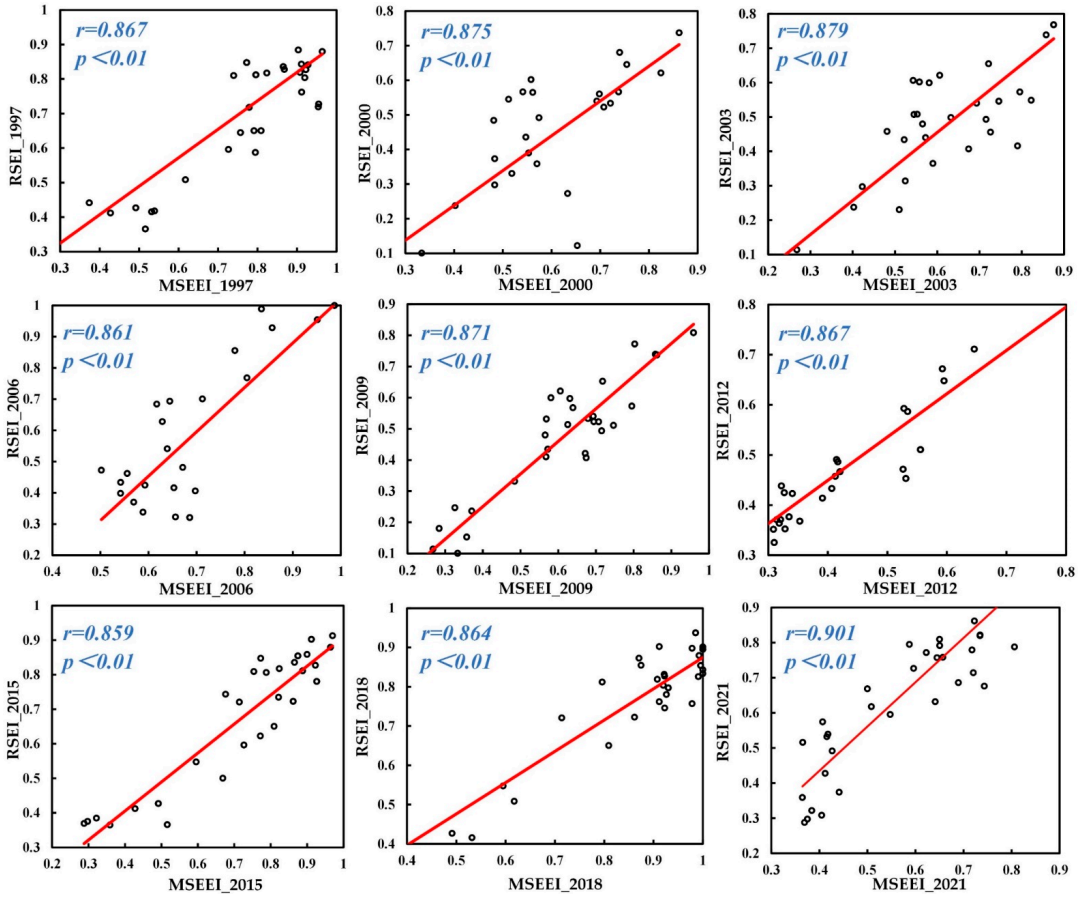


Figure 4. Correlations between the MSEEI and RSEI in 1997, 2000, 2003, 2006, 2009, 2012, 2015, 2018, and 2021.

Table 1. Mean correlations of the MSEEI and indicators.

Year	Mean Correlation of MSEEI and Indicators					
	EVI	**SMMI**	**NDBSI**	**DI**	**LST**	**MSEEI**
1997	0.916	0.852	0.919	0.853	0.781	0.942
2000	0.879	0.863	0.861	0.793	0.785	0.872
2003	0.831	0.824	0.856	0.879	0.793	0.892
2006	0.865	0.873	0.773	0.756	0.871	0.915
2009	0.887	0.794	0.803	0.817	0.835	0.894
2012	0.871	0.789	0.779	0.834	0.791	0.968
2015	0.815	0.827	0.781	0.864	0.879	0.889
2018	0.836	0.831	0.892	0.867	0.872	0.897
2021	0.871	0.845	0.906	0.854	0.862	0.923
Average	0.863	0.833	0.841	0.835	0.830	0.910

We counted the load values of the EVI, SMMI, NDBSI, DI, and LST on PC1 (Figure 5). The load values of the EVI and SMMI were always positive, indicating that EVI and SMMI had a positive effect on the ecological environment of the mining area. The load value of LST to PC1 was always negative, indicating that the NDBSI, DI, and LST had a negative effect on the ecological environment of the mining area. From 1997 to 2021, the load value of the EVI was in the range of 0.61~0.74, the positive effect of the EVI on the ecological environment of the mining area was relatively stable, the load range of the NDBSI was −0.42 to −0.55, the negative effect of the NDBSI on the ecological environment of the mining area was relatively stable. The load value of the DI ranged from −0.44 to −0.16, and the negative effect of the DI on the ecological environment first decreased and

then increased, which was relatively volatile. From 2003 to 2006, the load value of the SMMI decreased from 0.47 to 0.21, and the positive effect of the SMMI on the ecological environment of the mining area decreased significantly. From 2003 to 2012, the load value of LST increased from −0.29 to −0.04, and the negative effect of LST on the ecological environment of the mining area decreased. The effect was significantly weakened.

Table 2. Mean values of normalized ecological environment factors.

	1997	2000	2003	2006	2009	2012	2015	2018	2021
EVI	0.76	0.73	0.75	0.71	0.69	0.70	0.67	0.68	0.67
SMMI	0.69	0.66	0.67	0.64	0.59	0.56	0.57	0.55	0.54
NDBSI	0.40	0.37	0.43	0.32	0.47	0.39	0.41	0.38	0.36
DI	0.46	0.41	0.36	0.37	0.42	0.33	0.35	0.31	0.38
LST	0.31	0.37	0.33	0.35	0.40	0.41	0.32	0.36	0.34
MSEEI	0.85	0.82	0.83	0.81	0.79	0.77	0.80	0.84	0.80

3.2. Ecological Status of Mining Areas

The MSEEI results were graded (poor: 0 < MSEEI < 0.2; fair: 0.2 < MSEEI < 0.4; moderate: 0.4 < MSEEI < 0.6; good: 0.6 < MSEEI < 0.8; excellent: 0.8 < MSEEI < 1) (Figure 6). The ecological quality of the Luanchuan mining area was relatively good in 1997. After 1997, the overall ecological quality of the Luanchuan mining area declined compared with that in 1998, mainly because human engineering activities were closely related to prospecting and mining activities, and the original vegetation was replaced by open-pit mining. In 2021, the area with a poor ecological grade was 14.57 km^2, an increase of 12.4 km^2 from 1997; the area with a poor ecological grade was 7.79 km^2, an increase of 4.53 km^2 from 1997, and the area with a moderate ecological grade was 13.66 km^2, an increase of 0.80 km^2 from 1997. The area with a good grade was 87.22 km^2, which was 2.25 km^2 larger than that in 1997, and the ecologically unchanged area was 124.59 km^2, which was 19.97 km^2 smaller than that in 1997 (Figure 7).

We chose mining scopes with the same mining time as the research time to analyze the ecological status within mining scopes. Among the different sub-mining scopes of the Luanchuan mine, the open-pit mining Luotuoshan sulfur polymetallic mine scope (1.83 km^2), the open-pit mining Sandaozhuang molybdenum mine scope (2.51 km^2), the open-pit mining Qiushuigou mining area lead-molybdenum mine scope (9.27 km^2), and Zazigou Lead-Molybdenum Mine (2.05 km^2) were further selected to demonstrate mining activity intensification, and the original vegetation was replaced by open-pit mining sites, causing a deterioration in the ecological environment within the mining scopes (Figure 8). The mean value of the MSEEI within the mining scopes decreased with increasing years (Figure 9), which was consistent with the ecological conditions within the scopes (Figure 8). Comparison of the severity of ecological deterioration at the scale of scopes were ranked as follows: Sandaozhuang Molybdenum Mine > Zazigou Pb-Molybdenum Mine > Luotuoshan Sulfur-Polymetallic Mine > Qiushuigou Pb-Molybdenum Mine (Table 3).

Table 3. MSEEI values in each grade percentage of mining scopes.

Mining Scope		MSEEI in Each Grade Percentage (%)								
		1997	2000	2003	2006	2009	2012	2015	2018	2021
Qiushuigou Lead-Molybdenum Mine (9.27 km^2)	Poor	0.29	0.88	1.35	1.31	2.39	6.74	6.04	10.79	12.82
	Fair	0.64	0.48	0.36	0.95	2.90	6.39	3.27	3.96	4.25
	Moderate	4.68	0.65	0.54	2.90	4.02	6.42	3.90	7.61	7.29
	Good	30.08	18.12	18.26	27.16	28.53	36.70	17.51	33.41	25.39
	Excellent	64.30	79.87	79.49	67.67	62.16	43.75	69.27	44.23	50.26

Table 3. *Cont.*

Mining Scope		MSEEI in Each Grade Percentage (%)								
		1997	**2000**	**2003**	**2006**	**2009**	**2012**	**2015**	**2018**	**2021**
Luotuoshan Sulfur Polymetallic Mine (1.83 km^2)	Poor	0.29	14.97	15.47	8.76	14.92	10.82	11.68	19.53	18.21
	Fair	0.64	3.70	4.52	7.65	13.23	11.93	7.98	7.57	8.15
	Moderate	4.66	5.14	8.68	12.09	13.58	8.97	9.34	11.47	9.33
	Good	29.94	37.97	31.18	49.28	45.79	43.44	38.13	45.41	42.09
	Excellent	64.48	38.21	40.15	22.21	13.97	24.85	32.87	16.02	22.22
Sandaozhuang Molybdenum Mine (2.51 km^2)	Poor	18.49	21.58	22.20	47.13	69.91	72.99	73.05	79.62	78.21
	Fair	7.29	2.53	3.14	11.11	14.14	12.66	6.51	4.88	5.67
	Moderate	9.40	2.73	3.90	9.48	7.23	6.89	4.90	6.53	5.49
	Good	25.63	11.05	8.74	15.75	7.48	6.81	10.91	7.47	7.29
	Excellent	39.20	62.11	62.02	16.52	1.24	0.65	4.64	1.51	3.34
Zazigou Lead-Molybdenum Mine (2.05 km^2)	Poor	0.27	0.68	1.01	0.14	15.56	26.24	27.54	43.64	31.26
	Fair	1.33	0.40	0.36	0.54	3.56	6.62	4.07	4.94	8.94
	Moderate	8.23	1.08	1.04	1.52	5.56	3.20	3.35	7.78	12.67
	Good	31.57	22.71	25.88	22.92	27.57	36.39	19.51	23.22	20.81
	Excellent	58.60	75.13	71.71	74.87	47.75	27.54	45.54	20.42	26.32

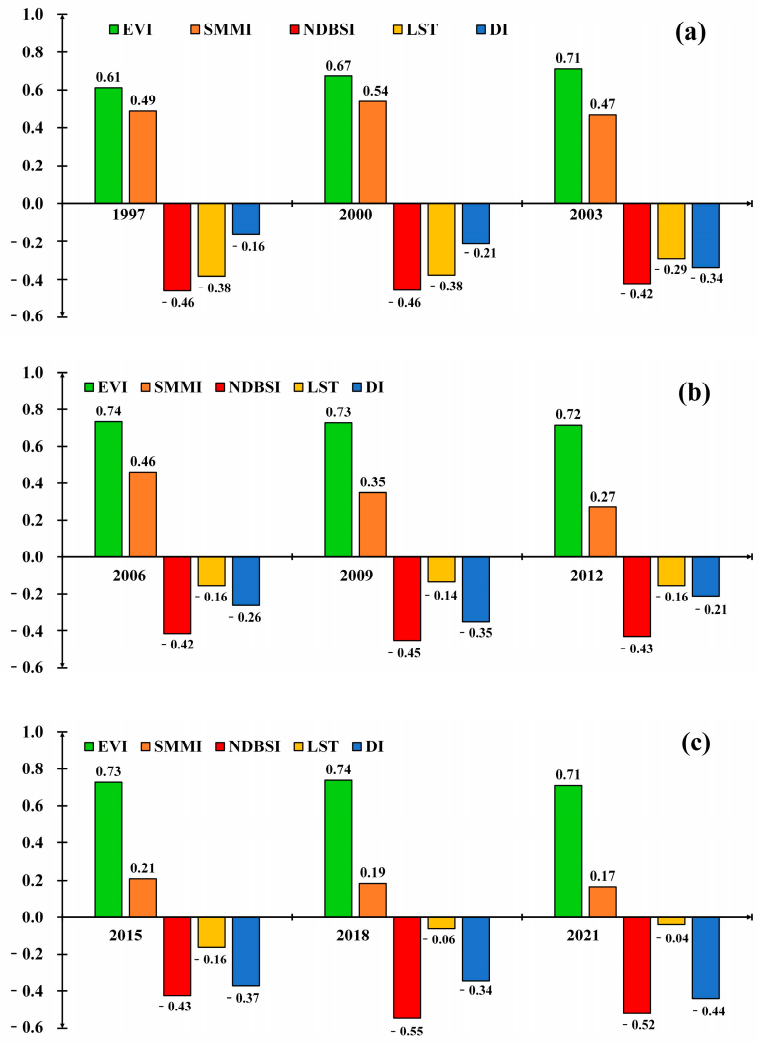


Figure 5. The EVI, SMMI, NDBSI, LST, and DI load on PC1 in 1997, 2000, 2003 (**a**); the EVI, SMMI, NDBSI, LST, and DI load on PC1 in 2006, 2009, 2012 (**b**); the EVI, SMMI, NDBSI, LST, and DI load on PC1 in 2015, 2018, 2021 (**c**).

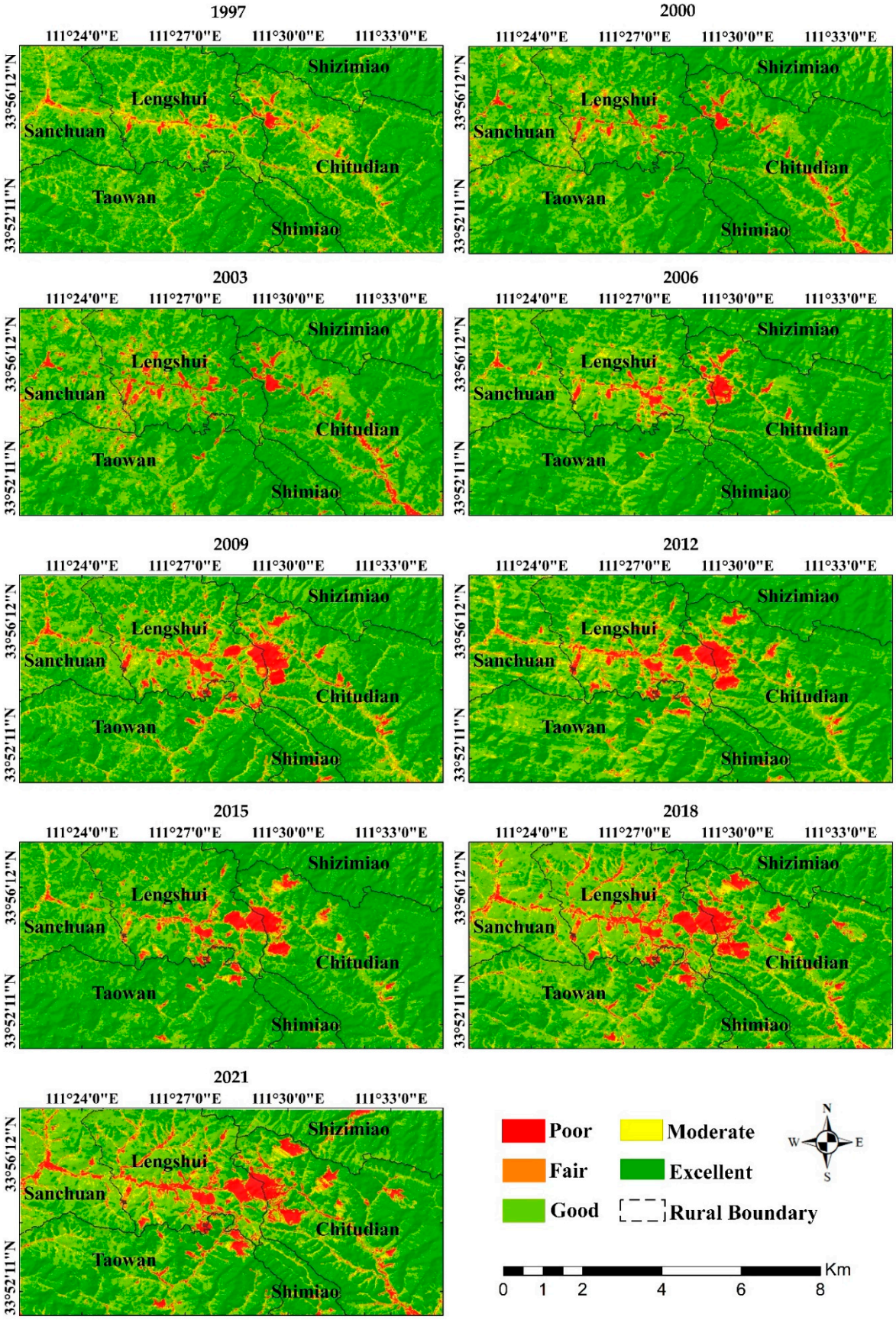


Figure 6. Ecological statuses of mining areas in 1997, 2000, 2003, 2006, 2009, 2012, 2015, 2018, and 2021.

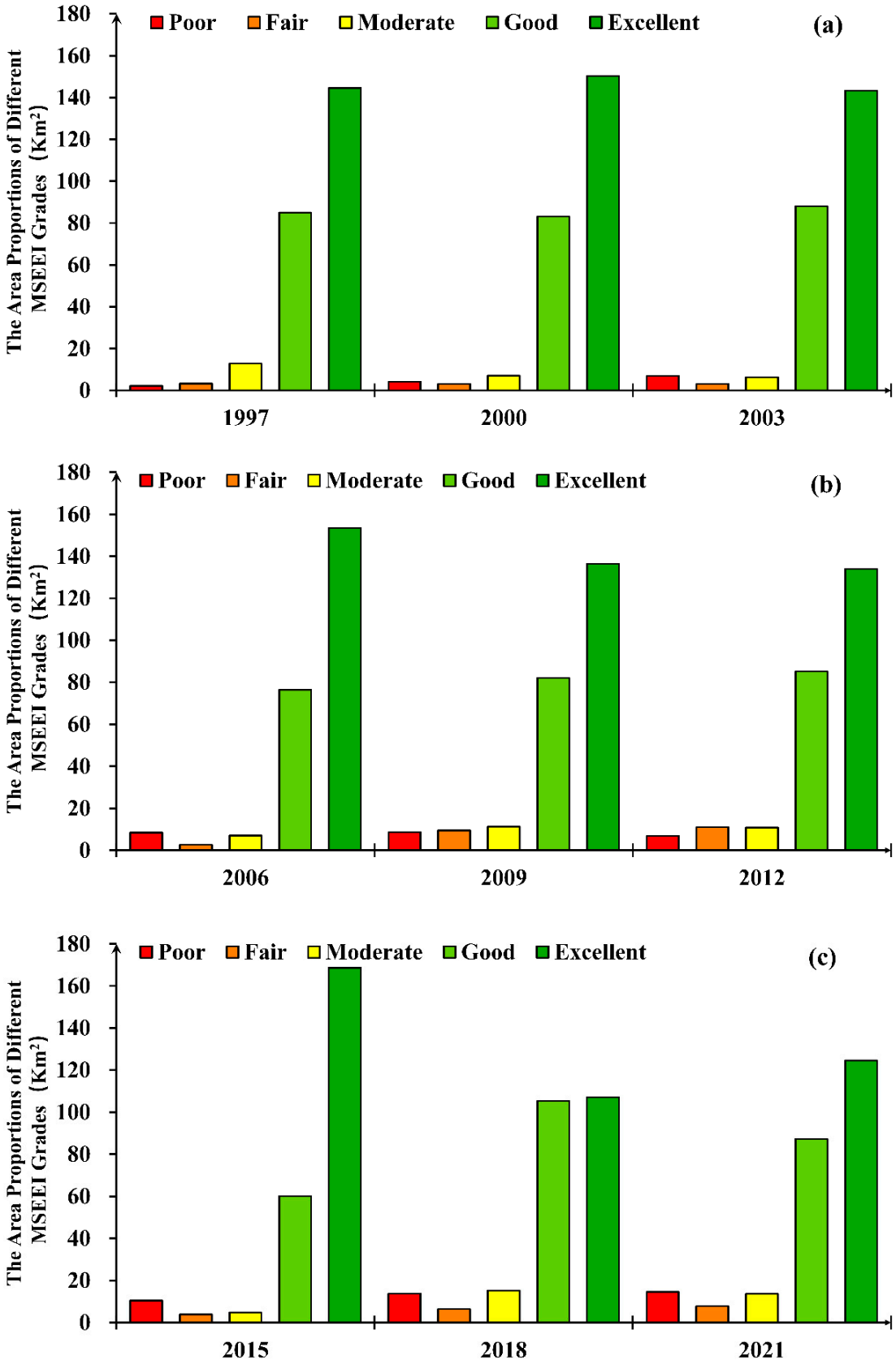


Figure 7. Areas of the ecological statuses of mining areas in 1997, 2000, 2003 (**a**); areas of ecological status of mining areas in 2006, 2009, 2012 (**b**); areas of ecological status of mining areas in 2015, 2018, 2021 (**c**).

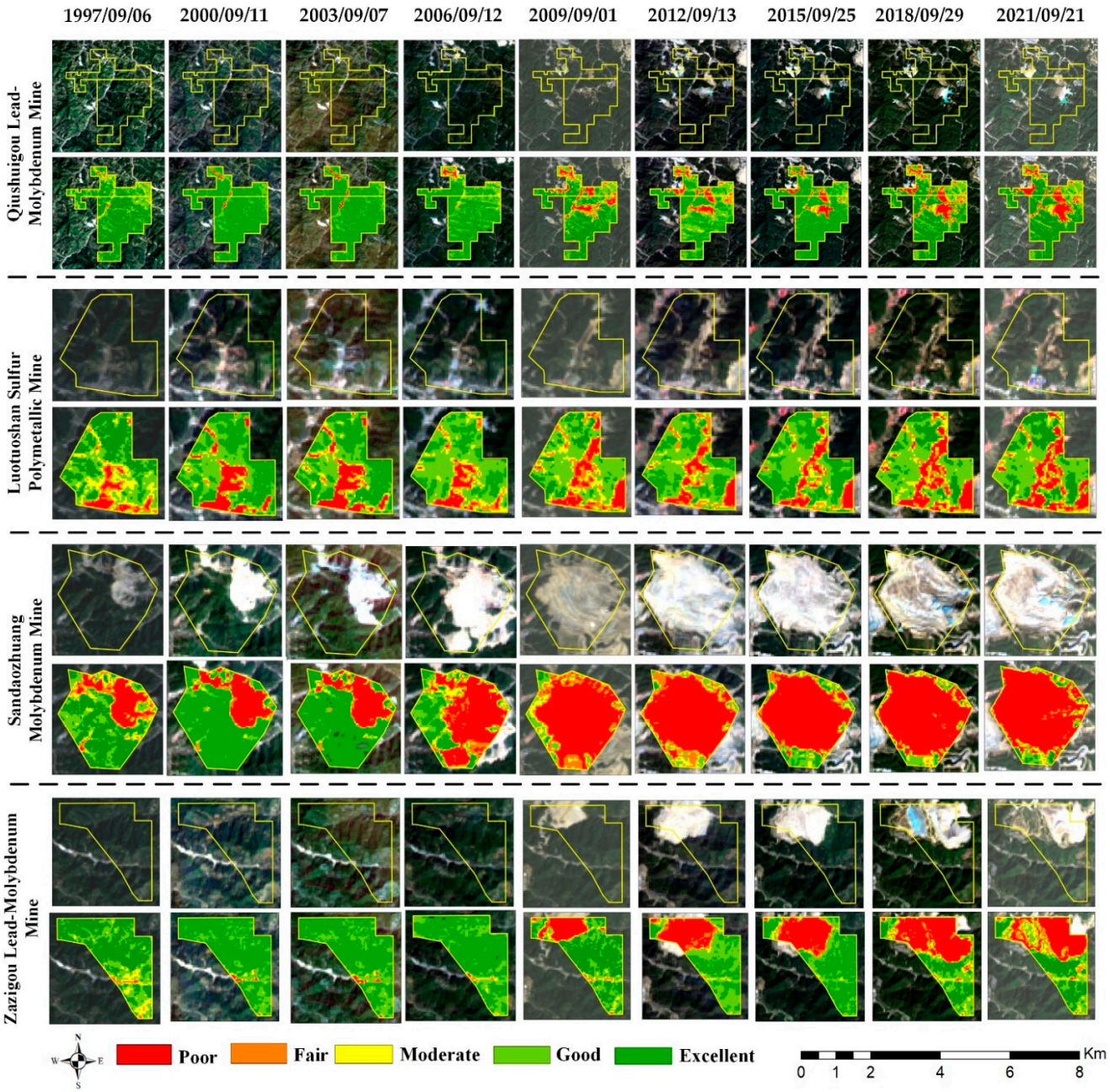


Figure 8. Ecological statuses for selected mining scopes in 1997, 2000, 2003, 2006, 2009, 2012, 2015, 2018, and 2021.

3.3. Ecological Changes in Mining Areas

We carried out the difference detection of ecological changes in the Luanchuan mining area (Figure 10). The detection results of the ecological difference in the mining area are divided into the following: Degraded (ΔMSEEI = −4, ΔMSEEI = −3, ΔMSEEI = −2, ΔMSEEI= −1), Unchanged (ΔMSEEI = 0), Improved (ΔMSEEI = 1, ΔMSEEI = 2, ΔMSEEI = 3, ΔMSEEI = 4) (Table 4). In 1997~2021, the deteriorated regions in the ecology of the Luanchuan mining area were concentrated in the southeast of Lengshui Town, the northwest of Chitudian Town and the northeast of Taowan Town; the ecologically improved areas were concentrated in the northeast of Chitudian Town. The Luanchuan mine concentration area suffered from ecological problems with the intensification of mining activities. Destruction and deterioration of the environment occurred, but under the guidance of the policy of development and governance, the ecology of some mining areas is gradually improving.

Table 4. MSEEI grades change detection from 1997 to 2021.

ΔMSEEI		Degraded			Unchanged			Improved		
		−4	−3	−2	−1	0	1	2	3	4
1997–2000	Area (km^2)	0.28	1.17	3.54	27.81	167.69	43.45	3.58	0.30	0.01
	Percentage (%)	0.11%	0.47%	1.43%	11.22%	67.66%	17.53%	1.44%	0.12%	0.00%
2000–2003	Area (km^2)	0.30	1.49	5.84	35.74	158.25	43.46	2.47	0.26	0.01
	Percentage (%)	0.12%	0.60%	2.36%	14.42%	63.85%	17.54%	1.00%	0.11%	0.00%
2003–2006	Area (km^2)	5.17	1.19	1.69	22.62	169.18	41.68	3.97	2.22	0.11
	Percentage (%)	2.09%	0.48%	0.68%	9.13%	68.26%	16.82%	1.60%	0.90%	0.04%
2006–2009	Area (km^2)	1.62	4.55	4.32	40.29	176.98	19.83	0.18	0.05	0.00
	Percentage (%)	0.65%	1.84%	1.74%	16.26%	71.41%	8.00%	0.07%	0.02%	0.00%
2009–2012	Area (km^2)	0.26	0.96	3.41	37.41	161.75	37.70	3.90	2.27	0.16
	Percentage (%)	0.10%	0.39%	1.38%	15.10%	65.27%	15.21%	1.57%	0.92%	0.07%
2012–2015	Area (km^2)	0.01	0.23	0.49	16.32	174.07	51.75	4.46	0.49	0.00
	Percentage (%)	0.00%	0.09%	0.20%	6.58%	70.24%	20.88%	1.80%	0.20%	0.00%
2015–2018	Area (km^2)	0.91	2.57	8.43	77.88	151.08	6.86	0.08	0.01	0.00
	Percentage (%)	0.37%	1.04%	3.40%	31.42%	60.96%	2.77%	0.03%	0.01%	0.00%
2018–2021	Area (km^2)	0.31	0.98	1.57	14.66	195.86	33.23	0.97	0.23	0.02
	Percentage (%)	0.12%	0.40%	0.63%	5.91%	79.03%	13.41%	0.39%	0.09%	0.01%
1997–2021	Area (km^2)	4.36	6.57	8.93	45.24	151.38	29.63	1.52	0.17	0.02
	Percentage (%)	1.76%	2.65%	3.60%	18.26%	61.08%	11.96%	0.61%	0.07%	0.01%

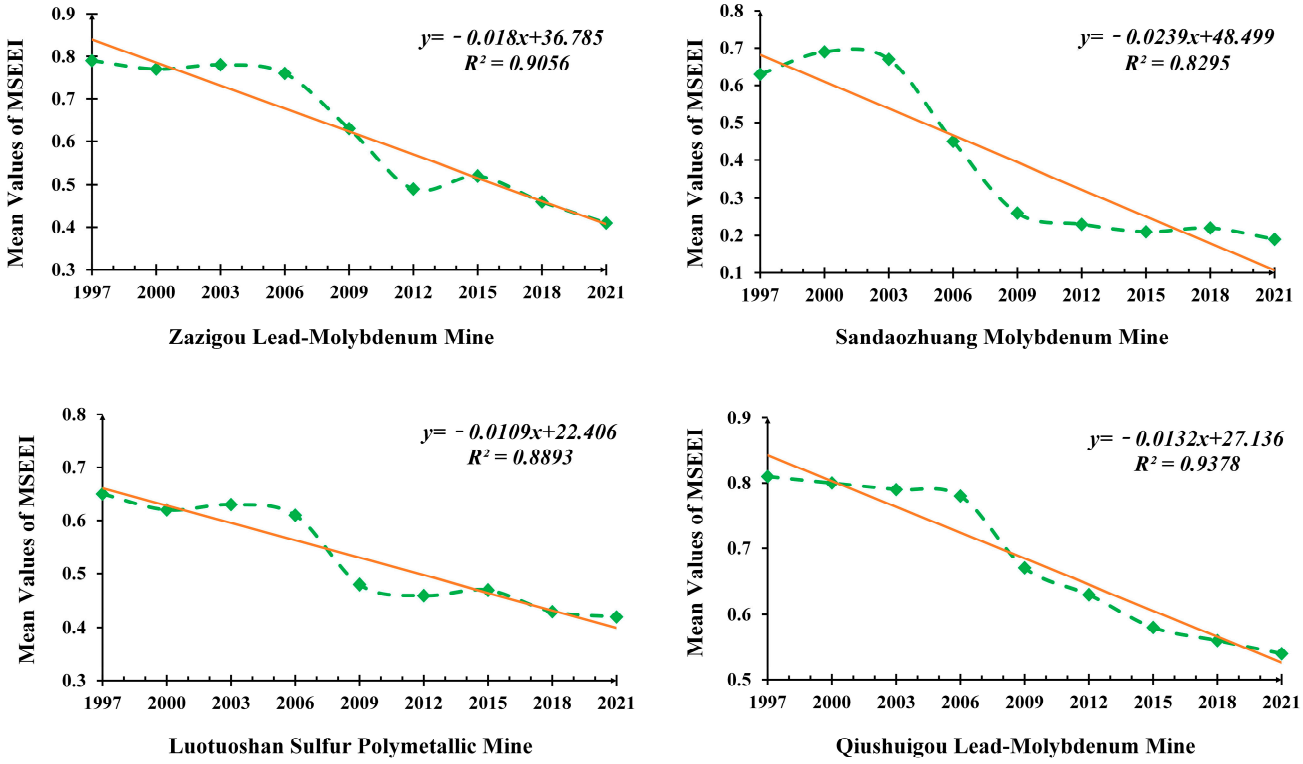


Figure 9. Mean values of the MSEEI for selected mining scopes in 1997, 2000, 2003, 2006, 2009, 2012, 2015, 2018, and 2021.

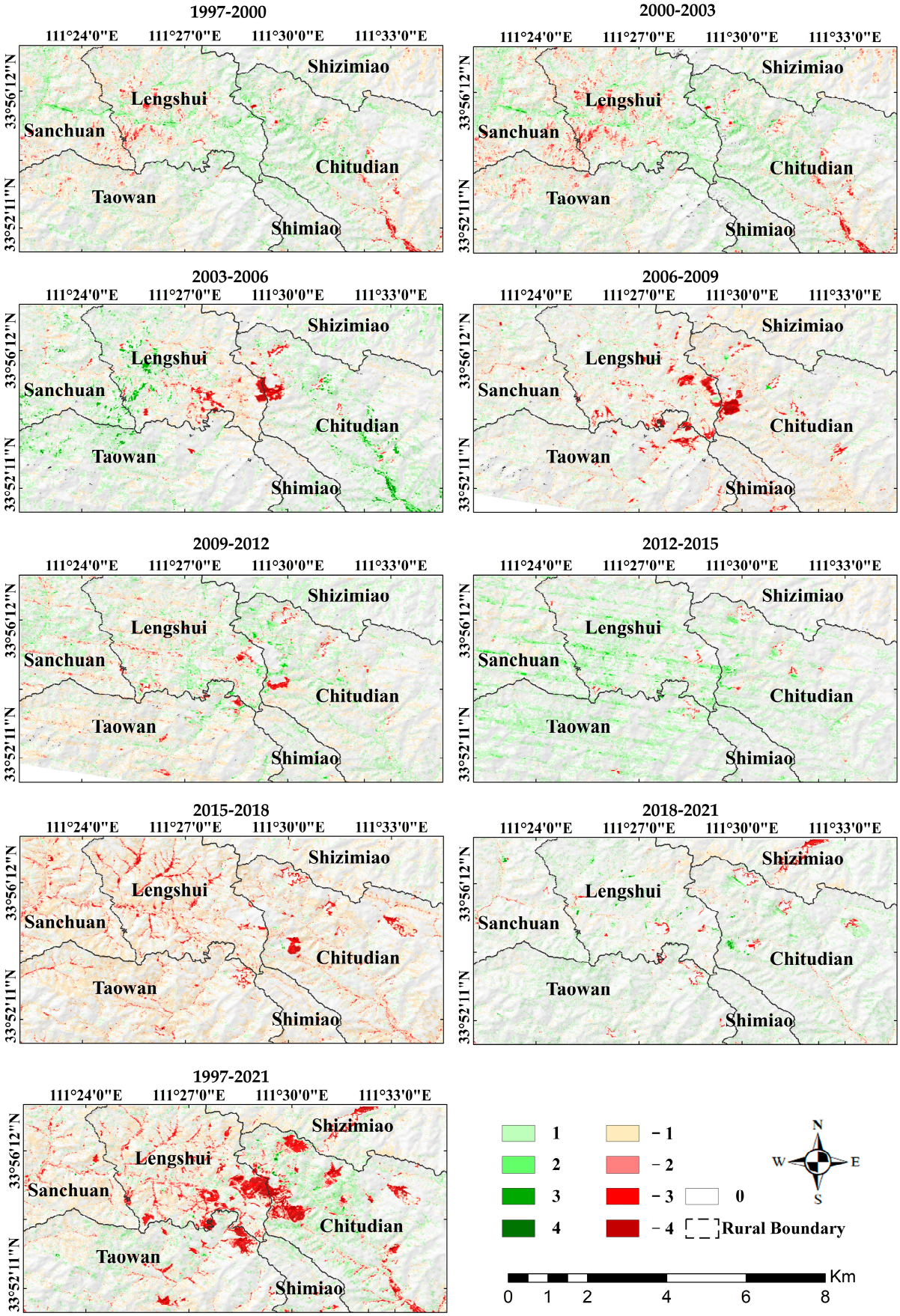


Figure 10. Ecological changes in mining areas in 1997, 2000, 2003, 2006, 2009, 2012, 2015, 2018, and 2021.

4. Discussion

4.1. MSEEI Provides an Effective Method for Assessing Mine Environments

Currently, the RSEI is widely used in regional ecological assessment research to assess the quality of the ecological environment in the long term. However, the RSEI is a generic environmental evaluation indicator, and not specifically designed for assessing mines [16,22,38,39]. In this study, by comprehensively considering the vegetation damage, soil drying, land cover change, surface temperature anomalies, air pollution, and other issues caused by mine development, a novel MSEEI was proposed through integrating the EVI, SMMI, NDBSI, LST, and DI. In order to verify the effect of the MSEEI in the ecological assessment of the mining area, we compared 1997 LANDSAT TM data, 2021 LANDSAT OLI data, Google images, and field survey photos in three regions with serious ecological deterioration. The results show that the serious ecological deterioration was mainly caused by expansions of the open pit, tailings pond, and waste dump during mining. The MSEEI could effectively reflect changes in the ecological environment during mining. The MSEEI inherited the principal component analysis method when constructed from the RSEI, and changed specific ecological indicators to adapt to the ecological environment assessment of the mining area. The MSEEI provides a new idea for the regional ecological assessment of mining areas, which can be widely used to assess the environmental grade of mining areas, and guide natural environment protection policies for mining areas.

4.2. MSEEI Change Patterns around the Ore Points

From 1997 to 2021, the ecological environment of the Luanchuan mining area changed greatly. We found that the lower the value of the MSEEI, the closer the area was to the boundary of open-pit mining (Figure 11), and the closer to the damage caused by the tailings pond, open-pit stope, dump, and concentrator to the surface ecological environment of the mining area, the lower the value of the MSEEI in the damaged area.

We analyzed the relationship between the change in ecological environment and the landform around the mine, and we analyzed the nuclear density of the mine site. According to the results of the nuclear density analysis, the area around the mine point is divided into five levels: the higher concentration area, the high concentration area, the medium concentration area, the low concentration area, and the lower concentration area (Figure 12). We made statistics on the DEM and MSEEI in different concentration areas (Table 5). The MSEEI value of the higher concentration area decreased from 0.84 to 0.78; the MSEEI value of the high concentration area decreased from 0.85 to 0.8; the MSEEI value of the medium concentration area decreased from 0.85 to 0.80; the MSEEI value of the low concentration area decreased from 0.85 to 0.83, and the MSEEI value of the lower concentration area decreased from 0.85 to 0.84. It shows that the ecological deterioration was more serious in the area where mines were concentrated.

Table 5. MSEEI in each grade percentage of regions.

Region	DEM (m)	Area Percentage of ΔMSEEI (%)								
		−4	−3	−2	−1	0	1	2	3	4
Higher concentration area (15.33 km^2)	828~1099	0.06	0.25	0.55	1.38	3.61	1.07	0.06	0.02	0.00
	1099~1283	0.58	0.53	0.48	3.00	14.13	4.43	0.24	0.01	0.00
	1283~1428	0.66	0.98	1.97	6.71	24.08	4.69	0.23	0.01	0.00
	1428~1685	0.38	0.60	0.64	6.68	19.34	2.54	0.08	0.00	0.00
High concentration area (11.93 km^2)	828~1099	0.34	0.55	0.73	1.33	4.81	1.69	0.12	0.02	0.00
	1099~1283	0.21	0.37	0.57	2.18	12.69	3.82	0.32	0.04	0.00
	1283~1428	0.70	1.65	2.28	8.08	22.89	5.18	0.29	0.03	0.00
	1428~1685	0.48	0.57	0.51	5.58	18.16	3.63	0.16	0.02	0.00

Table 5. *Cont.*

Region	DEM (m)	Area Percentage of ΔMSEEI (%)								
		−4	−3	−2	−1	0	1	2	3	4
Medium concentration area (24.86 km^2)	828~1099	0.12	0.32	0.71	2.06	7.76	2.65	0.17	0.03	0.00
	1099~1283	0.04	0.30	0.49	1.82	11.06	3.03	0.20	0.01	0.00
	1283~1428	1.71	2.35	2.46	8.32	19.85	4.21	0.32	0.03	0.00
	1428~1685	2.49	1.97	0.86	6.33	15.24	2.95	0.14	0.00	0.00
Low concentration area (42.28 km^2)	828~1099	0.53	0.62	0.60	1.39	3.27	1.17	0.03	0.00	0.00
	1099~1283	0.47	0.68	0.96	2.93	10.71	3.51	0.13	0.00	0.00
	1283~1428	1.84	3.26	2.25	6.28	19.35	4.12	0.20	0.06	0.04
	1428~1685	2.87	2.29	1.33	6.77	19.19	3.05	0.11	0.00	0.00
Lower concentration area (45.74 km^2)	828~1099	0.00	0.00	0.00	0.00	0.00	0.00	0.00	0.00	0.00
	1099~1283	0.15	0.37	0.84	2.30	8.46	4.11	0.60	0.14	0.05
	1283~1428	1.40	3.77	2.55	5.99	21.51	5.41	0.60	0.29	0.05
	1428~1685	0.67	0.89	0.82	3.05	30.48	5.29	0.22	0.00	0.00

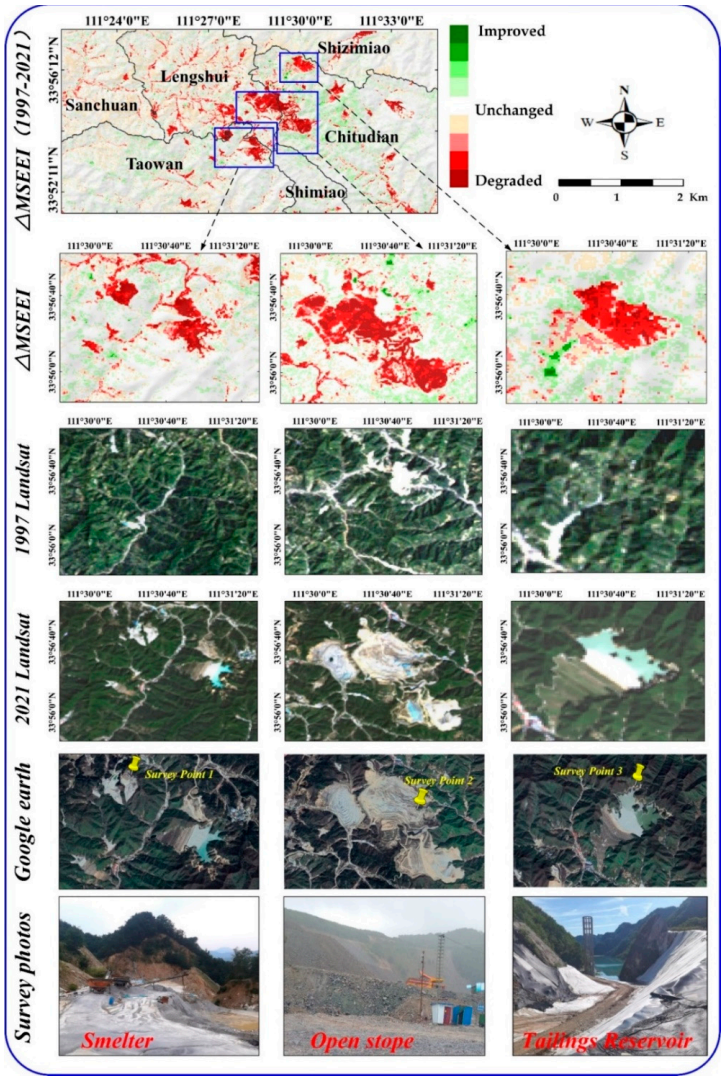


Figure 11. Field inspection and investigation of degraded areas.

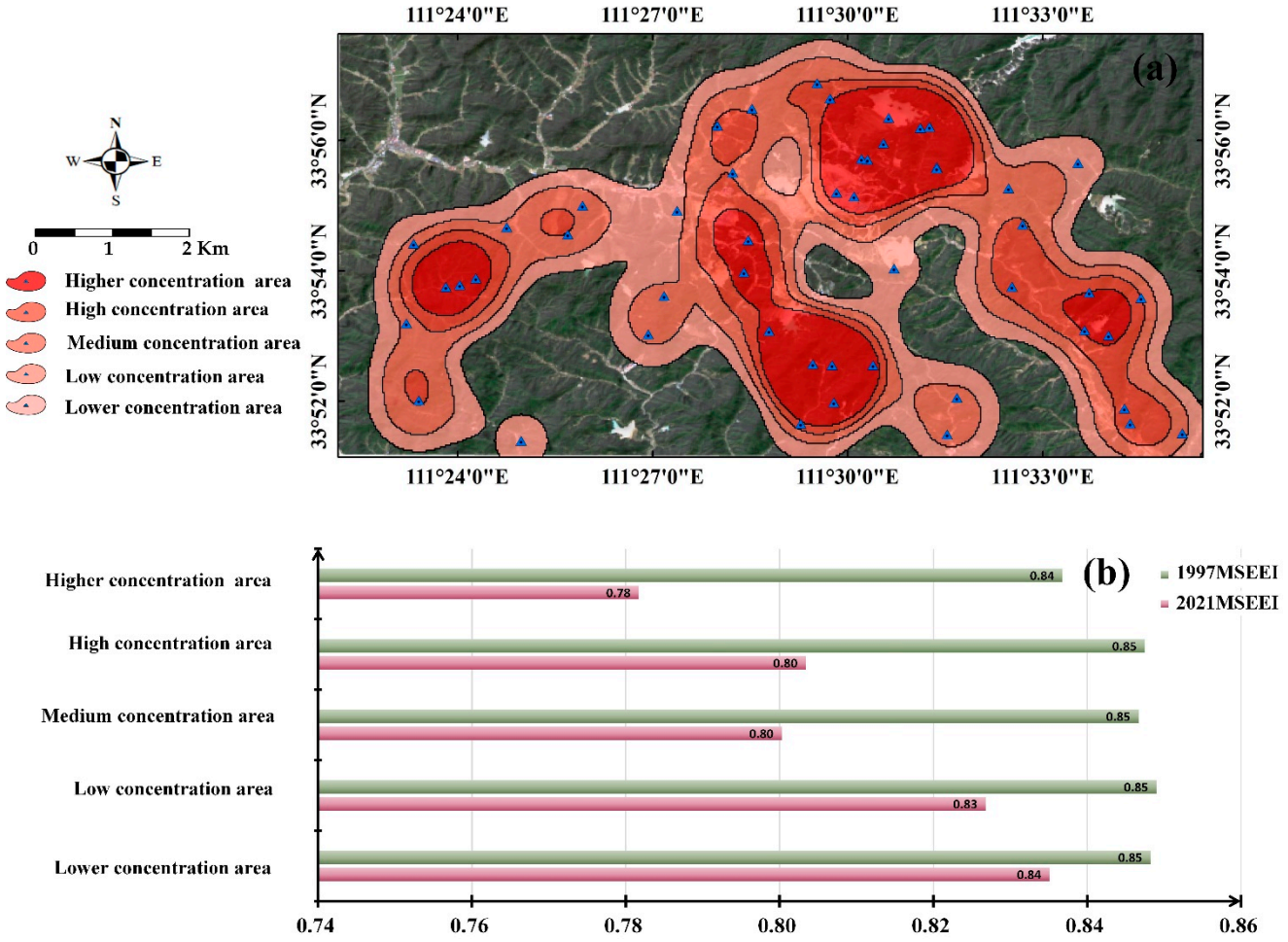


Figure 12. Nuclear density analysis diagram of mine points (**a**); MSEEI in 1997, 2021 (**b**).

In order to further illustrate the spatial pattern of the change in the MSEEI around ore points, an eight-directional fractal dimension was established, and the ore points of each dimension were counted (Table 6). By normalizing the MSEEI changes and the numbers of mining points of each type from 1997 to 2021, a radar chart of changes in the MSEEI and the number of mining points are obtained (Figure 13). It can be clearly seen that the MSEEI increases in the west, south, and east. If the change value of the MSEEI is greater than 0.5, there are few mining points in these three directions, the elevation is high, the vegetation is dense, the self-healing ability of the ecological environment is strong, and it is less affected by human engineering activities; on the contrary, the distribution of mining points in other directions is relatively dense, the vegetation is severely damaged and the ecological environment is poor. Artificial ecological restoration projects are needed to improve the quality of the ecological environment in the mining area.

Table 6. Statistics of the eight-center latitude ore points and the mean values of MSEEI change.

Direction	North	Northeast	East	Southeast	South	Southwest	West	Northwest
Pyrite	1	0	0	1	0	0	0	0
Gold mine	0	0	0	0	0	0	1	0
Molybdenum ore	0	4	1	0	1	0	0	0
Iron ore	0	0	0	0	0	0	0	0
Lead ore	5	2	5	4	1	0	0	1

Table 6. *Cont.*

Direction	North	Northeast	East	Southeast	South	Southwest	West	Northwest
Zinc ore	0	3	0	0	4	5	7	0
Total	6	9	6	5	6	5	8	1
Change Value	0.013	0.016	0.024	0.021	0.011	0.017	0.008	0.011

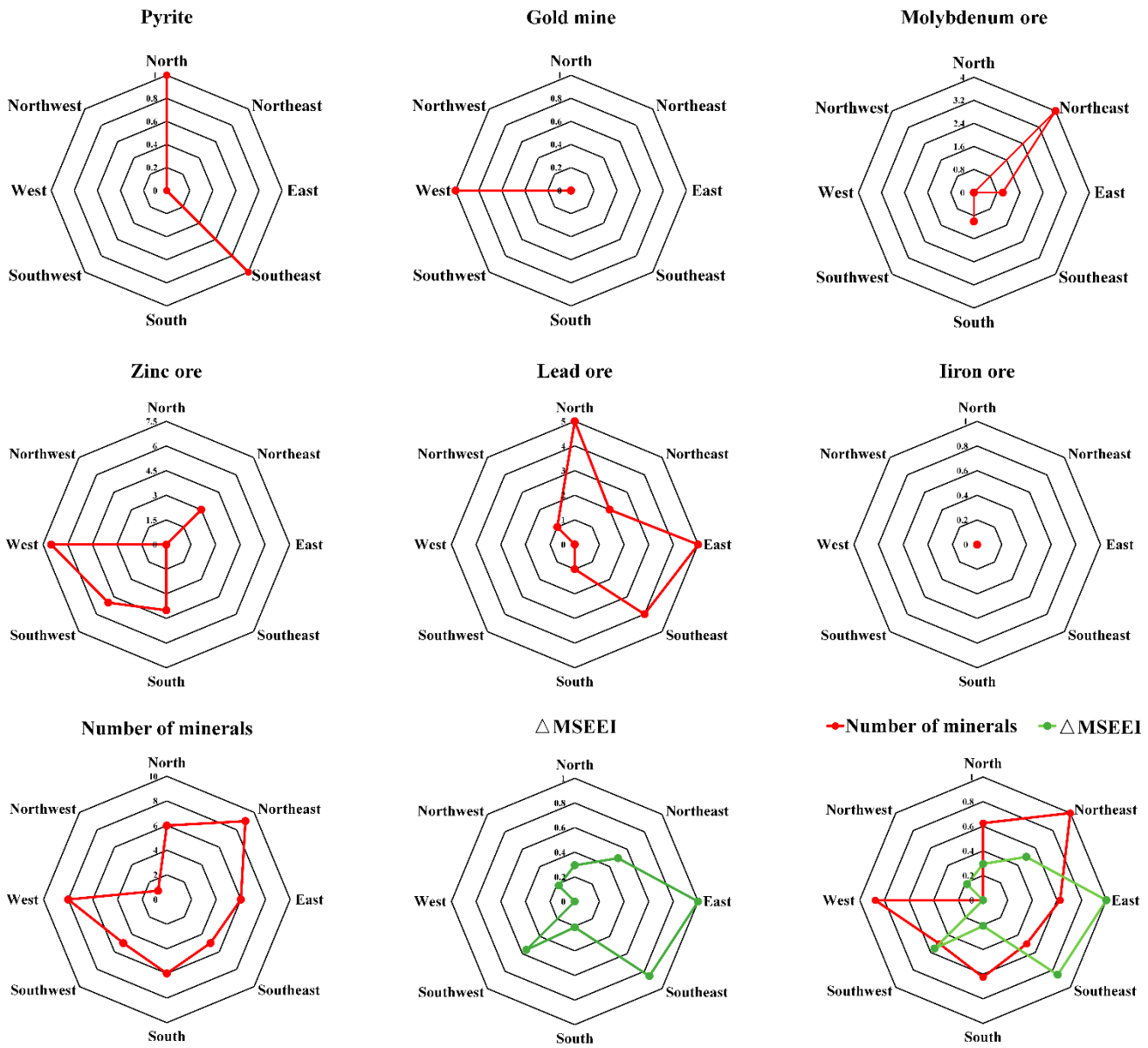


Figure 13. The spatial pattern of MSEEI change around the ore points.

4.3. Future Perspectives

From the perspective of ecological problems caused by mining, this study constructed the MSEEI, an index suitable for the regional evaluation of mining areas. The main research results can be used for long-term mine ecological environment assessment, ecological status assessment before and after mine treatment, and for the formulation of natural environmental protection policies for mines. However, there are also some shortcomings: (1) although the difference index DI can reflect regional PM2.5 concentration to a certain extent, its specific correlation needs to be further studied; (2) the ecological environment of a

mining area is affected by a variety of factors. In subsequent research, indexes such as water quality of the tailings pond, mining mode, mine wastewater pollution, biodiversity of the mining area, and carbon sequestration capacity should be included in the evaluation system.

5. Conclusions

Taking the Luanchuan mining cluster area in Luoyang City, Henan Province, as the research area, the Landsat satellite remote sensing image data and the mining point data of the Luanchuan mining cluster area in 1997, 2000, 2003, 2006, 2009, 2012, 2015, 2018, and 2021 were selected, and the remote sensing image data were used to extract the ecological impact factor constructs for the Mine-Specific Eco-Environment Index (MSEEI). Based on GIS spatial operation and spatial analysis, the ecological environment quality of the Luanchuan mining area was discussed.

The MSEEI is a kind of remote sensing index applicable to the ecological environment assessment of mining areas. The EVI and SMMI have a positive effect on the ecological environment of a mining area, while the NDBSI, DI, and LST have a negative effect on the ecological environment of a mining area. The overall ecological environment changes in the Luanchuan mining area showed local optimization and improvement, and overall decline. Among them, the mean MSEEI of the Sandaozhuang molybdenum mine, the Zhazigou lead-molybdenum mine and the Qiushuigou lead-molybdenum mine decreased more than 0.2, which caused the deterioration of the ecological environment within the mining rights. The area of ecological environment quality improvement in the mining area was 31.33 km^2, accounting for 12.65% of the ore concentration area. The area of deterioration of the ecological environment quality was 65.10 km^2, accounting for 26.27% of the total area of the city. The constant area occupied 151.38 km^2 or less. The area of the ecological deterioration was concentrated in the southeast of Shushui Town, the northwest of Chitudian Town and the northeast of Taowan Town, while the area of ecological improvement was concentrated in the northeast of Chitudian Town, and the overall change trend was "worse in the east and better in the west." The tailings pond, open stope, dump, and concentrator caused by mining damage to the surface ecological environment of the mining area resulted in the regional MSEEI value being low. There was a certain correlation between the change in ecological environment quality of the mining area and the mine, and the ecological environment quality of the place, with a small number of mines being stable and basically good or excellent.

Author Contributions: Conceptualization, P.Z. and X.C.; methodology, X.C.; software, P.Z.; validation, P.Z., Y.R. and S.L.; formal analysis, P.Z.; investigation, D.S.; resources, X.C.; data curation, P.Z.; writing—original draft preparation, P.Z.; writing—review and editing, X.C.; visualization, P.Z. and Y.W.; supervision, X.C.; project administration, X.C.; funding acquisition, X.C. All authors have read and agreed to the published version of the manuscript.

Funding: This research received no external funding.

Data Availability Statement: The data are unavailable due to privacy or ethical restrictions.

Conflicts of Interest: The authors declare no conflict of interest.

References

1. Li, M.S. Ecological restoration of mineland with particular reference to the metalliferous mine wasteland in China: A review of research and practice. *Sci Total Environ.* **2006**, *357*, 38–53. [CrossRef] [PubMed]
2. Miao, Z.; Marrs, R. Ecological restoration and land reclamation in open-cast mines in Shanxi Province, China. *J. Environ. Manag.* **2000**, *59*, 205–215. [CrossRef]
3. Quanyuan, W.; Jiewu, P.; Shanzhong, Q.; Yiping, L.; Congcong, H.; Tingxiang, L.; Limei, H. Impacts of coal mining subsidence on the surface landscape in Longkou city, Shandong Province of China. *Environ. Earth Sci.* **2009**, *59*, 783–791. [CrossRef]
4. Tripathi, N.; Singh, R.S. Ecological restoration of mined-out areas of dry tropical environment, India. *Environ. Monit Assess* **2008**, *146*, 325–337. [CrossRef]
5. Xiao, W.; Zhang, W.; Ye, Y.; Lv, X.; Yang, W. Is underground coal mining causing land degradation and significantly damaging ecosystems in semi-arid areas? A study from an Ecological Capital perspective. *Land Degrad. Dev.* **2020**, *31*, 1969–1989. [CrossRef]

6. Zhang, M.; Wang, J.; Li, S. Tempo-spatial changes and main anthropogenic influence factors of vegetation fractional coverage in a large-scale opencast coal mine area from 1992 to 2015. *J. Clean. Prod.* **2019**, *232*, 940–952. [CrossRef]
7. Chaka, D.S.; Oda, T.K. Understanding land surface temperature on rift areas to examine the spatial variation of urban heat island: The case of Hawassa, southern Ethiopia. *GeoJournal* **2019**, *86*, 993–1014. [CrossRef]
8. Guan, Y.; Wang, J.; Zhou, W.; Bai, Z.; Cao, Y. Identification of land reclamation stages based on succession characteristics of rehabilitated vegetation in the Pingshuo opencast coal mine. *J. Environ. Manag.* **2022**, *305*, 114352. [CrossRef]
9. Ma, C.; Guo, Z.-z.; Zhang, X.-k.; Han, R.-m. Annual integral changes of time serial NDVI in mining subsidence area. *Trans. Nonferrous Met. Soc. China* **2011**, *21*, s583–s588. [CrossRef]
10. Przeździecki, K.; Zawadzki, J.J. Triangle method modification with second degree polynomial edges fitting in LST NDVI scatterplot in lignite mine influence area. *Remote Sens. Appl. Soc. Environ.* **2020**, *20*, 100404. [CrossRef]
11. Thakur, T.K.; Dutta, J.; Upadhyay, P.; Patel, D.K.; Thakur, A.; Kumar, M.; Kumar, A. Assessment of land degradation and restoration in coal mines of central India: A time series analysis. *Ecol. Eng.* **2022**, *175*, 106493. [CrossRef]
12. Zhang, B.; Wu, D.; Zhang, L.; Jiao, Q.; Li, Q. Application of hyperspectral remote sensing for environment monitoring in mining areas. *Environ. Earth Sci.* **2011**, *65*, 649–658. [CrossRef]
13. MORAIN, S.A. Commercialization of remote-sensing technology. *Int. J. Remote Sens.* **2016**, *6*, 837–846. [CrossRef]
14. Airiken, M.; Zhang, F.; Chan, N.W.; Kung, H.T. Assessment of spatial and temporal ecological environment quality under land use change of urban agglomeration in the North Slope of Tianshan, China. *Environ. Sci. Pollut. Res. Int.* **2022**, *29*, 12282–12299. [CrossRef]
15. Hang, X.; Li, Y.; Luo, X.; Xu, M.; Han, X. Assessing the Ecological Quality of Nanjing during Its Urbanization Process by Using Satellite, Meteorological, and Socioeconomic Data. *J. Meteorol. Res.* **2020**, *34*, 280–293. [CrossRef]
16. Hu, X.; Xu, H. A new remote sensing index for assessing the spatial heterogeneity in urban ecological quality: A case from Fuzhou City, China. *Ecol. Indic.* **2018**, *89*, 11–21. [CrossRef]
17. Jiang, F.; Zhang, Y.; Li, J.; Sun, Z. Research on remote sensing ecological environmental assessment method optimized by regional scale. *Environ. Sci. Pollut. Res. Int.* **2021**, *28*, 68174–68187. [CrossRef]
18. Jing, Y.; Zhang, F.; He, Y.; Kung, H.-t.; Johnson, V.C.; Arikena, M. Assessment of spatial and temporal variation of ecological environment quality in Ebinur Lake Wetland National Nature Reserve, Xinjiang, China. *Ecol. Indic.* **2020**, *110*, 105874. [CrossRef]
19. Liu, H.; Jiang, Y.; Misa, R.; Gao, J.; Xia, M.; Preusse, A.; Sroka, A.; Jiang, Y. Ecological environment changes of mining areas around Nansi lake with remote sensing monitoring. *Environ. Sci. Pollut. Res. Int.* **2021**, *28*, 44152–44164. [CrossRef]
20. Liu, Q.; Yang, Z.; Han, F.; Shi, H.; Wang, Z.; Chen, X. Ecological Environment Assessment in World Natural Heritage Site Based on Remote-Sensing Data. A Case Study from the Bayinbuluke. *Sustainability* **2019**, *11*, 6385. [CrossRef]
21. Maity, S.; Das, S.; Pattanayak, J.M.; Bera, B.; Shit, P.K. Assessment of ecological environment quality in Kolkata urban agglomeration, India. *Urban Ecosyst.* **2022**, *25*, 1137–1154. [CrossRef]
22. Ning, L.; Jiayao, W.; Fen, Q. The improvement of ecological environment index model RSEI. *Arab. J. Geosci.* **2020**, *13*, 403. [CrossRef]
23. Qureshi, S.; Alavipanah, S.K.; Konyushkova, M.; Mijani, N.; Fathololomi, S.; Firozjaei, M.K.; Homaee, M.; Hamzeh, S.; Kakroodi, A.A. A Remotely Sensed Assessment of Surface Ecological Change over the Gomishan Wetland, Iran. *Remote Sens.* **2020**, *12*, 2989. [CrossRef]
24. Xu, H.; Wang, Y.; Guan, H.; Shi, T.; Hu, X. Detecting Ecological Changes with a Remote Sensing Based Ecological Index (RSEI) Produced Time Series and Change Vector Analysis. *Remote Sens.* **2019**, *11*, 2345. [CrossRef]
25. Wingate, V.; Phinn, S.; Kuhn, N.; Bloemertz, L.; Dhanjal-Adams, K. Mapping Decadal Land Cover Changes in the Woodlands of North Eastern Namibia from 1975 to 2014 Using the Landsat Satellite Archived Data. *Remote Sens.* **2016**, *8*, 681. [CrossRef]
26. Gallay, M.; Mora, A.; Martinez, J.-M.; Gardel, A.; Laraque, A.; Sarrazin, M.; Beaucher, E.; Doudou, J.-C.; Lagane, C. Dynamics and fluxes of organic carbon and nitrogen in two Guiana Shield river basins impacted by deforestation and mining activities. *Hydrol. Process.* **2018**, *32*, 17–29. [CrossRef]
27. Katpatal, Y.B.; Patil, S.A. Spatial analysis on impacts of mining activities leading to flood disaster in the Erai watershed, India. *J. Flood Risk Manag.* **2010**, *3*, 80–87. [CrossRef]
28. Wei, X.Q.; Gu, X.F.; Meng, Q.Y.; Yu, T.; Jia, K.; Zhan, Y.L.; Wang, C.M. Cross-Comparative Analysis of GF-1 Wide Field View and Landsat-7 Enhanced Thematic Mapper Plus Data. *J. Appl. Spectrosc.* **2017**, *84*, 829–836. [CrossRef]
29. Yan, X.; Qiao, X.; Yang, S.; Feng, M.; Song, X.; Zhang, M.; Xiao, L.; Zhang, Z.; Shafiq, F.; Yang, W.; et al. Hyperspectral response and monitoring study of soil moisture content based on the optimized spectral index. *Soil Sci. Soc. Am. J.* **2022**. [CrossRef]
30. Xu, S.; Miao, Y.; Li, Y.; Zhou, Y.; Ma, X.; He, Z.; Zhao, B.; Wang, S. What Factors Drive Air Pollutants in China? An Analysis from the Perspective of Regional Difference Using a Combined Method of Production Decomposition Analysis and Logarithmic Mean Divisia Index. *Sustainability* **2019**, *11*, 4650. [CrossRef]
31. Rousta, I.; Olafsson, H.; Nasserzadeh, M.H.; Zhang, H.; Krzyszczak, J.; Baranowski, P. Dynamics of Daytime Land Surface Temperature (LST) Variabilities in the Middle East Countries During 2001–2018. *Pure Appl. Geophys.* **2021**, *178*, 2357–2377. [CrossRef]
32. Qu, Y.; Chi, Y.; Gao, J.; Ma, X.; Wang, Y.P. Distinguishing the determinative landscape factors influencing the spatial variation of soil quality in Chongming Island, China. *J. Coast. Conserv.* **2022**, *26*, 42. [CrossRef]

33. Gou, R.; Zhao, J. Eco-Environmental Quality Monitoring in Beijing, China, Using an RSEI-Based Approach Combined With Random Forest Algorithms. *IEEE Access* **2020**, *8*, 196657–196666. [CrossRef]
34. Xie, S.; Jin, F.; Krishnan, S.; Sattar, F. Signal feature extraction by multi-scale PCA and its application to respiratory sound classification. *Med. Biol. Eng. Comput.* **2012**, *50*, 759–768. [CrossRef]
35. Falco, C.M.; Jiang, X.; Li, Y.; Chen, H.-L.; Song, B.-W.; Zhu, P.-L.; Zhang, H.-W. Vegetation pixels extraction based on red-band enhanced normalized difference vegetation index. In Proceedings of the Eighth International Conference on Digital Image Processing (ICDIP 2016), Chengdu, China, 20–23 May 2016.
36. Zhao, H.; Li, Y.; Chen, X.; Wang, H.; Yao, N.; Liu, F. Monitoring monthly soil moisture conditions in China with temperature vegetation dryness indexes based on an enhanced vegetation index and normalized difference vegetation index. *Theor. Appl. Climatol.* **2020**, *143*, 159–176. [CrossRef]
37. Arekhi, M. Investigating Land Surface Temperature (LST) Change Using the LST Change Detection Technique (Gomishan District, Iran). In *Advances in Remote Sensing and Geo Informatics Applications*; Advances in Science, Technology & Innovation; Springer: Cham, Switzerland, 2019; pp. 135–139.
38. Tang, H.; Fang, J.; Xie, R.; Ji, X.; Li, D.; Yuan, J. Impact of Land Cover Change on a Typical Mining Region and Its Ecological Environment Quality Evaluation Using Remote Sensing Based Ecological Index (RSEI). *Sustainability* **2022**, *14*, 12694. [CrossRef]
39. Xu, F.; Li, H.; Li, Y. Ecological environment quality evaluation and evolution analysis of a rare earth mining area under different disturbance conditions. *Environ. Geochem. Health* **2021**, *43*, 2243–2256. [CrossRef]

Disclaimer/Publisher's Note: The statements, opinions and data contained in all publications are solely those of the individual author(s) and contributor(s) and not of MDPI and/or the editor(s). MDPI and/or the editor(s) disclaim responsibility for any injury to people or property resulting from any ideas, methods, instructions or products referred to in the content.